

Thermal fluctuation mitigation in the ESS cryogenic moderator system induced by proton beam injection or trip: cooling power control in preliminary commissioning

H Tatsumoto*, A Horvath, T Vasilopoulos, and I Haag

European Spallation Source (ESS) ERIC, Lund, Sweden

*E-mail: hideki.tatsumoto@ess.eu

Abstract. At the European Spallation Source (ESS), a large-scale 20 K helium refrigeration system, which is called Target Moderator CryoPlant (TMCP), provides a cooling capacity of 30.3 kW at 15 K. The TMCP is designed to cool the cryogenic moderator system (CMS), which includes hydrogen moderators, subject to a static heat load of 4.6 kW and dynamic heat load of 6.7 kW under a 5 MW proton beam. Subcooled liquid hydrogen at 17 K and 1.1 MPa is circulated through the moderators at 0.5 kg/s. A valve box, installed into the TMCP adjacent to the CMS cold box, adjusts the helium feed flow rate to regulate the cooling capacity required to compensate for dynamic heat load changes when the proton beams are injected or tripped. In this study, the cooling capacity control approach was experimentally evaluated using the valve box during preliminary CMS commissioning in 2024, where helium was used instead of hydrogen, and the moderators were not connected. The experimental results identified the optimal operational conditions for each proton beam power.

1. Introduction

At the European Spallation Source (ESS), long-pulsed cold and thermal neutron fluxes with very high brightness will be provided to the research community. A 2 GeV proton beam with a power of 5 MW is directed onto a rotating tungsten target wheel at a repetition of 14 Hz with a pulse length of 2.86 ms to produce high-energy spallation neutrons. The high-energy neutrons are slowed down to cold and thermal neutrons by the moderators, optimized for a high cold neutron brightness [1]. The resulting high brightness cold neutron beams will be delivered to scientific instruments for neutron scattering. Currently, two hydrogen moderators are positioned above the target wheel, with their nuclear heating estimated at 6.7 kW for the 5-MW proton beam power. In the future, these will be replaced by four moderators (two above and two below the target wheel), with a total estimated nuclear heating of 17.2 kW [2].

The ESS cryogenic moderator system (CMS) is designed to circulate subcooled liquid hydrogen at 17 K and 1.1 MPa using two hydrogen pumps arranged in parallel, as shown in Fig.1 [3]. The distribution lines to each moderator are configured in parallel to ensure uniform inlet temperatures at all moderators. The flow rate is specified as 0.5 kg/s for the current two-moderator configuration and 1.0 kg/s for the planned future four-moderator configuration, maintaining an average temperature rise of less than 3 K across each moderator. The heat load is



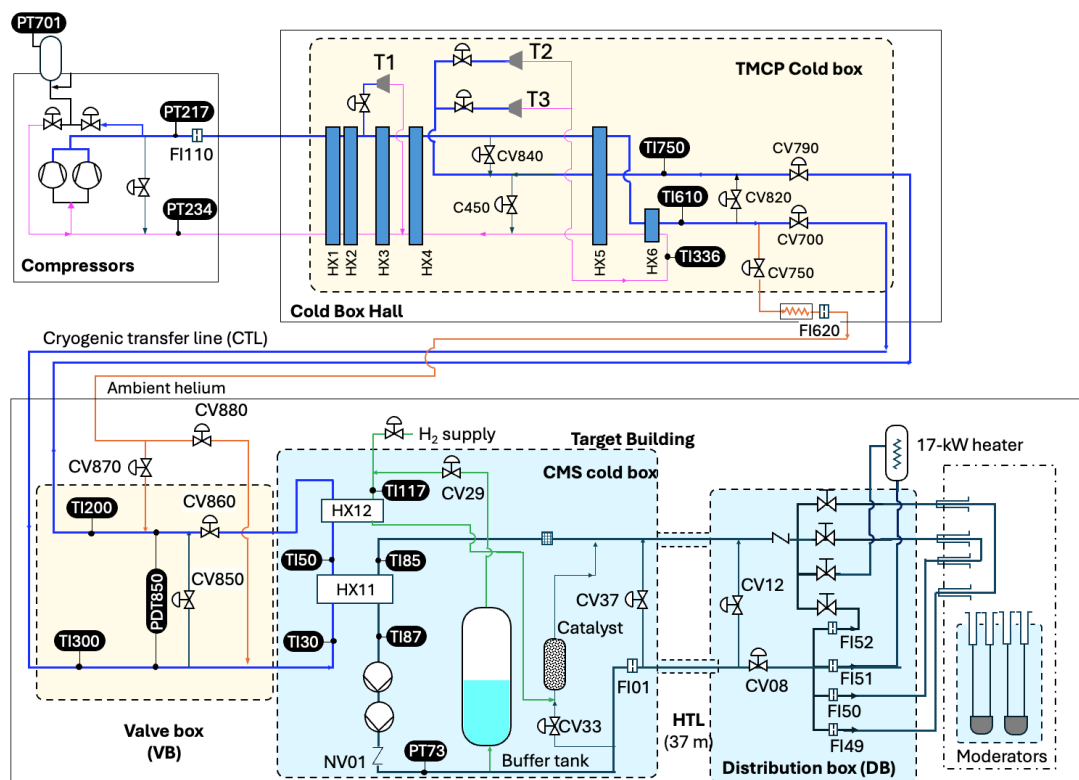


Figure 1. Overview of the cryogenic moderator system (CMS).

efficiently removed through a plate-fine type He-H₂ heat exchanger (HX11) located in the CMS cold box. This is cooled by the large-scale 20 K helium refrigeration system, the Target Moderator Cryoplant (TMCP), with a cooling capacity of 30.3 kW at 15 K [4]. The TMCP employs a floating pressure process [5] to control its cooling capacity, varying the discharge pressure (HP) from 0.7 to 2.0 MPa, while maintaining a constant compression ratio at 4.1. High-pressure helium flow at 16 K is delivered from the TMCP cold box to a valve box adjacent to the CMS cold box through a 300 m-vacuum insulated cryogenic helium transfer line (CTL) [6]. A temperature controller regulates the helium supply temperature (TI610) by operating two bypass valves (CV450 and CV840) for two cold parallel turbines (T2 and T3) using a split range control. A small fraction of the cooled HP stream, which is lower than 25 g/s measured by FI620, is warmed using an ambient heater (aluminum star fin tube vaporizer). The valve box adjusts both the helium supply temperature to the CMS cold box (TI30) and the helium return temperature (TI200) at 21.2 K via two mixing valves (CV880 and CV870) [7].

When proton beams are injected or tripped, the heat load associated with nuclear heating changes rapidly. To adjust the cooling power delivered to the CMS, the helium feed flow rate (\dot{m}_c) to the heat exchanger (HX11) is regulated, by CV860 while the bypass valve (CV850) is automatically adjusted to maintain a constant pressure drop across the bypass line, as measured by PDT850. This control scheme enables the TMCP cold box to operate with a constant cooling power. The two parallel expansion turbines are located downstream of the return CTL (R-CTL) to maintain a high-density helium stream in the supply CTL (S-CTL). This approach reduces the heat load in the CTL by allowing the use of smaller process diameters.

Tatsumoto et al. [8] developed a simulation model of the heat exchanger to investigate the propagation of thermal fluctuations from the CMS to the TMCP caused by proton beam injection

or trip. The simulation results provided insights into the required ramping-up and down speeds of the feed flow rate and the appropriate timing to initiate the ramp-up or ramp-down operation.

In this study, the cooling capacity control approach was experimentally evaluated using CV860 and CV850 during preliminary CMS commissioning in 2024, where helium was used instead of hydrogen, and the CMS was not connected to the moderators. The experimental results identified the optimal operational conditions corresponding to each proton beam power.

2. Adjusting the delivered cooling capacity

2.1 Estimation of the flow rate via the CTL

Under nominal conditions, all turbines (T1, T2, and T3) were operated. Each turbine was equipped with its own controller to regulate the turbine speed near the point of the maximum efficiency and to calculate the corresponding mass flow rate. During the previous TMCP commissioning conducted in 2022 [7], the mass flow rates calculated by each turbine controller (\dot{m}_{T1} , \dot{m}_{T2} , and \dot{m}_{T3}) were calibrated using a reference flow meter (FI100) (\dot{m}_{100}) [7].

In the present commissioning, with CV450 operating between 50% and 85% open, the flow rates through the S-CTL (\dot{m}_S) and R-CTL (\dot{m}_R) were expressed in terms of the mixing flow rate through CV870 (\dot{m}_w), which was measured using the flow meter (FI620). During the test, the other mixing valve (CV880) remained closed.

$$\dot{m}_R = \dot{m}_{100} - \dot{m}_{T1} \quad (1)$$

$$\dot{m}_S = \dot{m}_R - \dot{m}_w \quad (2)$$

Additionally, the flow rate through the R-CTL (\dot{m}_R) could also be determined from the measured mixing flow rate (\dot{m}_w) and the corresponding temperatures, using a thermal balance at the mixing point downstream of CV870.

$$\dot{m}_R = \frac{h_w - h_{400}}{h_{200} - h_{400}} \dot{m}_w \quad (3)$$

where h presents the enthalpy, and the subscripts of 200, 400 and w correspond to the locations of TI200, TI400 and T_w , respectively.

Figure 2 compares \dot{m}_R estimated using Eq. (1) with that calculated from the thermal balance in Eq. (3). The flow rates to the TMCP cold box (\dot{m}_{100}) were varied by adjusting the compressor discharge pressure (HP), which was gradually increased and decreased between 0.96 MPa and 1.4 MPa at a slow ramp speed of 0.8 kPa/min during the measurement. The flow rates derived from Eq. (1) aligned with those obtained from Eq. (3) within $\pm 2\%$ error. This agreement suggests that the flow rate through T1 (\dot{m}_{T1}) was estimated accurately. These results indicate the potential to predict both the flow rate through the bypass line via CV850 (\dot{m}_b) and the flow rate supplied to HX11 (\dot{m}_c), using the estimated flow rates (\dot{m}_S and \dot{m}_R) from Eq. (1) and Eq. (3).

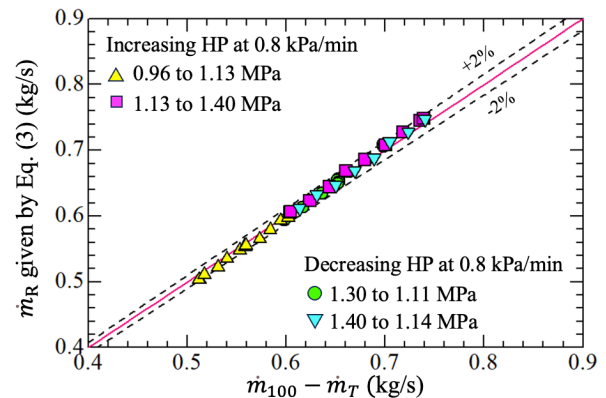


Figure 2. Comparison of \dot{m}_R estimated using Eq. (1) with that by Eq. (3).

2.2 Estimation of the flow rate via CV850

The cooling power delivered to the CMS is adjusted by regulating the helium feed flow rate (\dot{m}_c) to the heat exchanger (HX11) via the return valve (CV860). Simultaneously, the bypass valve (CV850) is controlled by a PID controller to maintain a consistent pressure drop (ΔP_b) across the bypass line, as measured by PDT850. This control approach ensures that the pressure drop across the entire CTLs remained constant, thereby supporting stable TMCP operation. In addition, the return CTL temperature (TI200) is maintained at 21.2 K by mixing helium gas through CV870. As a result, adjustments to the TMCP cooling power are unnecessary, as the temperature and pressure distributions in the R-CTL remain unchanged. Accurate estimation of \dot{m}_c and \dot{m}_b is essential for the effective implementation of this control approach. However, the absence of flow meters in the valve box prevents direct measurement. To estimate \dot{m}_b , the pressure drop (ΔP_b) and the valve position of CV850 were utilized. Figure 3 shows the measured Kv values for CV850, which has a specified value of 52 and a rangeability of 100:1 at 290 K, with CV860 fully closed. The bypass flow rates (\dot{m}_b) were measured using a flow meter (FI110), with all turbines out of operation. The measured Kv values at pressures of 1.14, 1.22 and 1.48 MPa followed the same trend, indicating pressure independence. However, the maximum Kv observed at a 100% valve opening was lower than the specified value of 52. Additionally, the measured values were lower than those estimated using the measured Kv of 38, based on the 100:1 rangeability. To improve the accuracy of \dot{m}_b estimation, a fitting curve representing the actual characteristics of CV850 was derived.

Figure 4 shows the behavior of the bypass valve (CV850) as the return valve (CV860) was gradually closed from 80% to 52%, while maintaining ΔP_b of 9.0 kPa. The flow rate through the S-CTL (\dot{m}_s) was 0.539 kg/s, at 16.5 K and 1.04 MPa. The position of CV850 was automatically adjusted by a PID controller. Although ΔP_b temporarily exceeded the setpoint of 9.0 kPa during changes in the CV860 position, the controller continued regulating CV850. The bypass flow rates (\dot{m}_b) were calculated using the Kv fitting curve for CV850 derived in Fig. 3, which allowed the estimation of \dot{m}_c as $\dot{m}_s - \dot{m}_b$. Similar to Eq. (3), the flow rate through CV850 (\dot{m}_b) can be expressed in terms of \dot{m}_w and \dot{m}_R , based on a thermal balance.

$$\dot{m}_b = \frac{\dot{m}_R(h_{200} - h_{400}) - \dot{m}_w(h_w - h_{400})}{h_{300} - h_{400}} \quad (4)$$

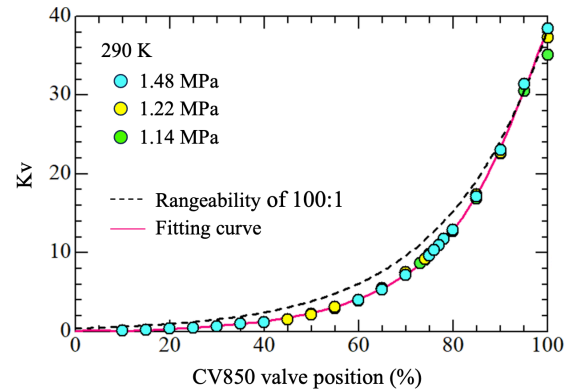


Figure 3. Measured Kv value for CV850.

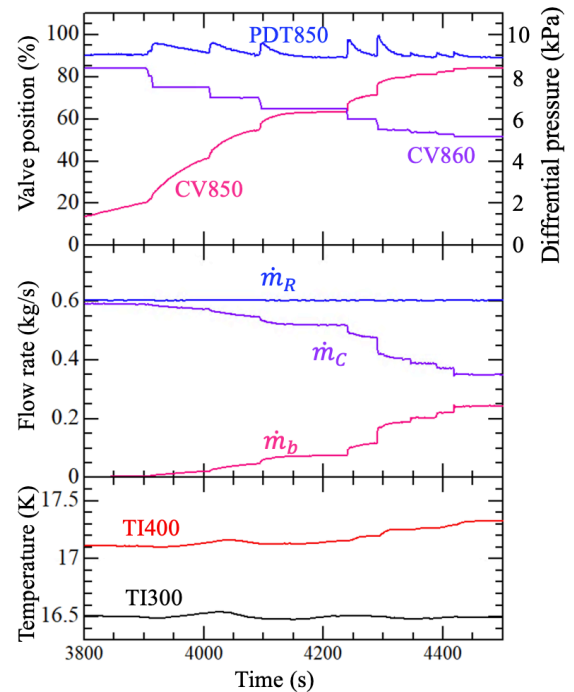


Figure 4. Comparison of the flow rates through the R-CTL estimated using Eq. (1) with those by Eq. (3).

As shown in Fig. 5, \dot{m}_b estimated using the measured Kv agreed with those obtained from the thermal balance within $\pm 10\%$ error. This result demonstrates the effectiveness of the proposed approach for predicting \dot{m}_b .

2.3 Stable operational conditions

The helium flow rate of 0.2 kg/s through the heat exchanger (HX11) is required during the beam trip to remove the static heat load and maintain the hydrogen supply temperature (TI87) at 17.0 K. Tatsumoto et al. [8] developed a one-dimensional simulation model of HX11 to analyze the propagation of thermal fluctuations from the CMS to the

TMCP. The simulation results indicated that, to adjust the cooling capacity in response to the dynamic heat load and maintain the hydrogen supply temperature at 17.0 K when the 2 MW and 5 MW proton beams were injected, the helium feed flow rate must increase by an additional 0.156 kg/s and 0.252 kg/s, respectively. Furthermore, to mitigate fluctuations in the hydrogen supply temperature (TI87) within ± 0.1 K, ramping speeds of the helium feed flow rate in the range of 0.03 to 0.08 (kg/s)/s were found to be necessary for 2 MW proton beam operation, and

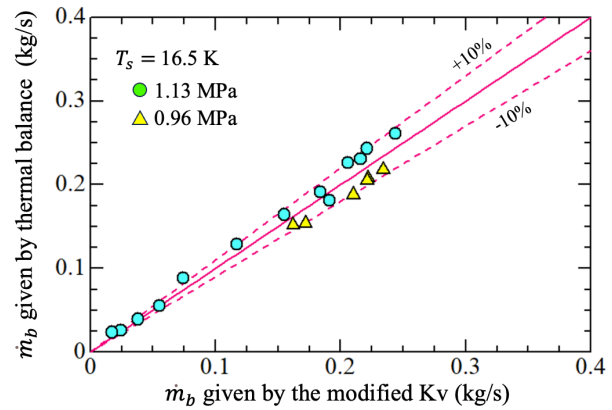
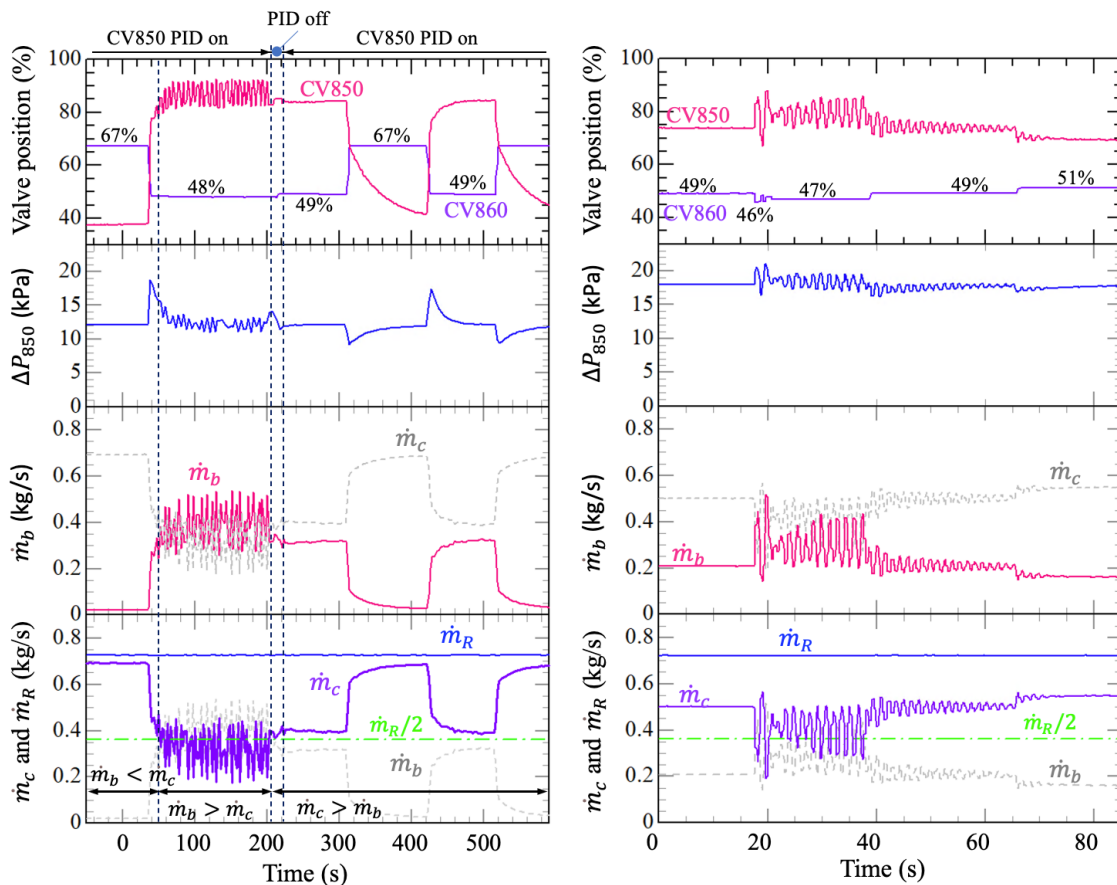


Figure 5. Bypass flow rates through CV850 compared with those calculated from the thermal balance.



(a) Closing CV860 from 67% to 48%

(b) Closing CV860 by a few %

Figure 6. Behaviors of CV850, PDT850, and estimated distribution flow rates during changing in CV860.

0.06 to 0.1 (kg/s)/s for 5 MW operation. Figure 6 (a) shows the behaviors of the bypass valve (CV850), differential pressure (ΔP_b), and the distribution of the estimated low rates (\dot{m}_b and \dot{m}_c) when the return valve (CV860) was rapidly adjusted between 67% and 48% at a ramp rate of 4%/s under a pressure of 1.39 MPa. Following the closure of CV860 from 67% to 49%, CV850 responded smoothly, and ΔP_b stabilized around the setpoint of 12.2 kPa, although a temporary increase in ΔP_b was observed due to a delay in the PID control response of CV850. In contrast, when CV860 was reopened from 49% to 67%, ΔP_b temporarily decreased before returning the setpoint. The time required for CV850 to stabilize was noticeably longer after CV860 was opened than after it was closed. 72% of the total change in CV850 was achieved within 5 seconds, corresponding to a ramping flow rate of 0.041 (kg/s)/s. However, when CV860 was closed from 67% to 48%, which was just 1% below the previous position of 49%, CV850 exhibited sustained oscillations that did not subside. To eliminate the oscillation, the PID control function for CV850 was temporarily deactivated, and CV860 was adjusted back to 49%, where the oscillation had not been observed. After reactivating the PID function, the oscillation did not occur. To further investigate the stability limit of the CV850 PID control, CV860 was changed by 1% to 2% around the position of 49%, as shown in Fig. 6 (b). When CV860 was decreased from 49% to 46%, CV850 exhibited oscillations with an amplitude variation of $\pm 10\%$. As CV860 was increased from 46%, the oscillations were gradually suppressed and completely disappeared at 51%. These test results indicated that oscillations in CV850 occurred when \dot{m}_c dropped below \dot{m}_b . In other words, to avoid instability when reducing \dot{m}_c , it must be maintained above $\dot{m}_s/2$ ($=\dot{m}_b$).

Figure 7 shows the effect of the HP (PT217) on \dot{m}_s and \dot{m}_R , as well as on ΔP_b , under the conditions where CV850 was fully closed (0%) and CV860 was fully opened (100%). Both the flow rates and pressure drop increased proportionally with the pressure. As described in Eq. (2), the difference between \dot{m}_s and \dot{m}_R corresponds to the mixing flow rate (\dot{m}_w) through CV870, which serves to maintain the R-CTL temperature (TI200) at 21.2 K. For instance, at a pressure of 1.6 MPa, \dot{m}_w is approximately 13 g/s. The setpoint of PDT850 should be set above ΔP_b . However, as shown in Fig. 8, the maximum allowable CV850 position, which was estimated using the calculated $\dot{m}_{b,max}$ ($=\dot{m}_s/2$), ΔP_b for CV850 = 0% and CV860 = 100%, and the measure Kv characteristics presented in Fig. 3, was found to be approximately 87.8%, regardless of the pressure range from 1.0 MPa to 1.8 MPa.

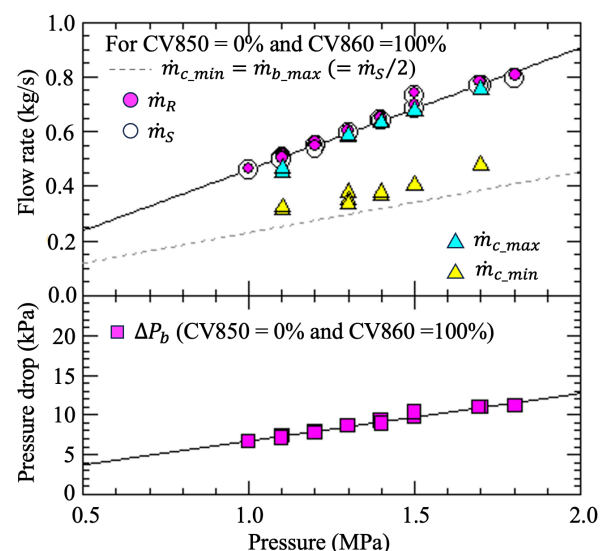


Figure 7. Effect of the HP (PT217) on \dot{m}_s and \dot{m}_R and ΔP_b .

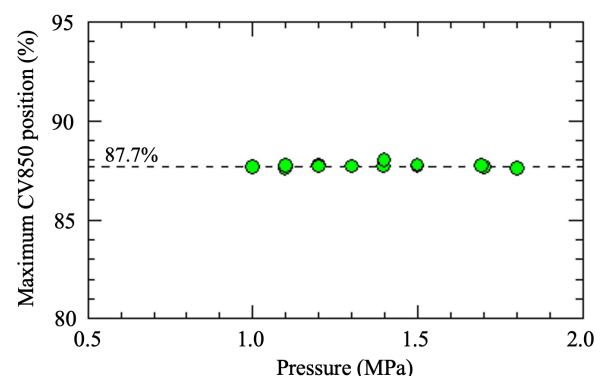


Figure 8. Maximum allowable CV850 position.

2.4 Test results of approach to adjusting the delivered cooling power

Figure 9 shows the behaviors of CV850, ΔP_b , \dot{m}_b and \dot{m}_c at pressures of 1.1, 1.4 and 1.7 MPa, when the return valve (CV860) was suddenly opened and closed, without exceeding the CV850 limitations of 87.7% described in Fig. 8. The PDT850 setpoints (ΔP_{sp}) were configured as follows: set to 6.4 kPa at HP = 1.1 MPa, 10.2 kPa at HP = 1.4 MPa, and 13.1 kPa at HP = 1.7 MPa. No oscillations in CV850 were observed after CV860 was closed, as the position of CV850 was maintained at approximately 83%. As the pressure increased, both \dot{m}_R and \dot{m}_c also increased. The allowable maximum variation in \dot{m}_c , which corresponded to $\dot{m}_c/2$, also became more pronounced, even though the required movement of CV860 became smaller. The effects of HP on the maximum and minimum allowable values of \dot{m}_c (\dot{m}_{c_max} and \dot{m}_{c_min}) are shown in Fig. 7. The upper and lower limits increased proportionally with HP and closely matched \dot{m}_s and $\dot{m}_s/2$, respectively, as previously described. These results indicated that HP levels of 0.77 MPa and 1.1 MPa were required to adjust the cooling capacity in response to the dynamic heat loads for 2 MW and 5 MW proton beam operations, respectively.

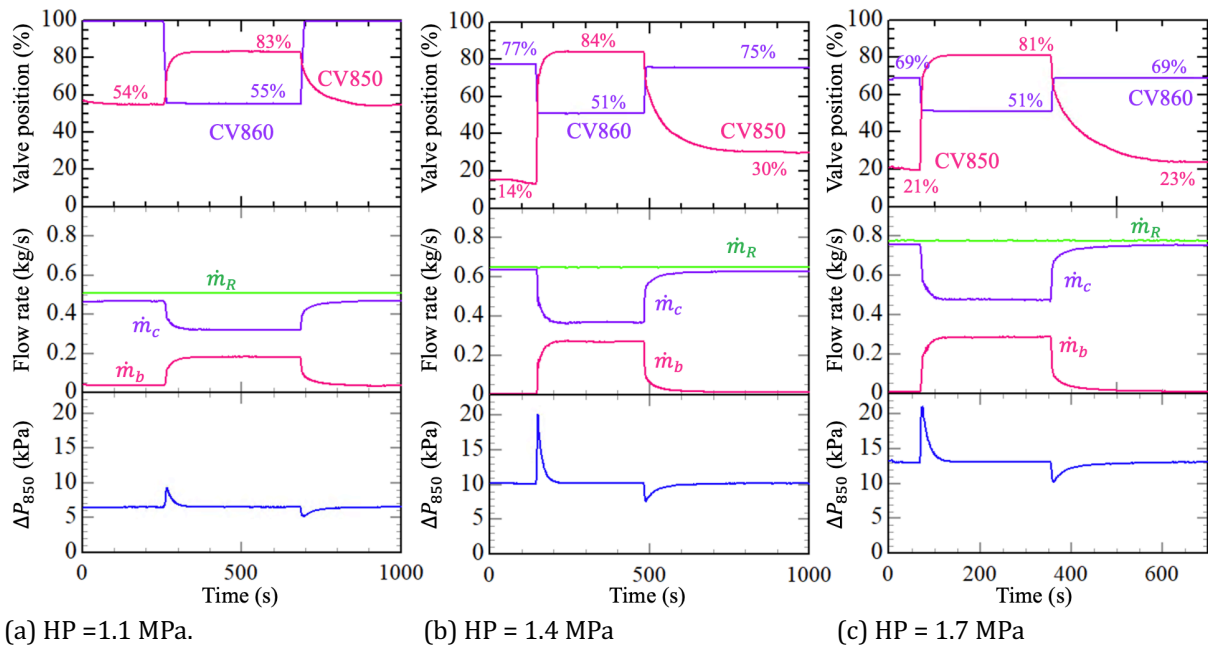


Figure 9. Predicted maximum allowable position of CV850.

Figure 10 shows the effect of CV860 ramp-up and ramp-down speeds on \dot{m}_c and \dot{m}_b at a pressure of 1.5 MPa. The ramp speeds were set to 1.0, 2.0, and 5.6%/s, with 5.6%/s being the maximum ramp speed, limited by the actuator's movement capability. No fluctuations were observed at the ramp speeds, although a temporary deviation in ΔP_b was noted due to the time delay in the PID control response. The CV860 ramp speeds of 1.0, 2.0, and 5.6%/s corresponded to \dot{m}_c ramp rates of 0.012, 0.02, 0.09 (kg/s)/s, respectively. These test results demonstrated that the movement capability of the CV860 actuator satisfied the required ramp rate ranges of 0.03 to 0.08 (kg/s)/s for 2 MW proton beam operation, and 0.06 to 0.09 (kg/s)/s for 5 MW proton beam operations [8].

3. Conclusions

The cooling capacity control approach was experimentally evaluated using the bypass valve (CV850) and the supply valve (CV860) in the TMCP valve box. When CV860 was closed, CV850

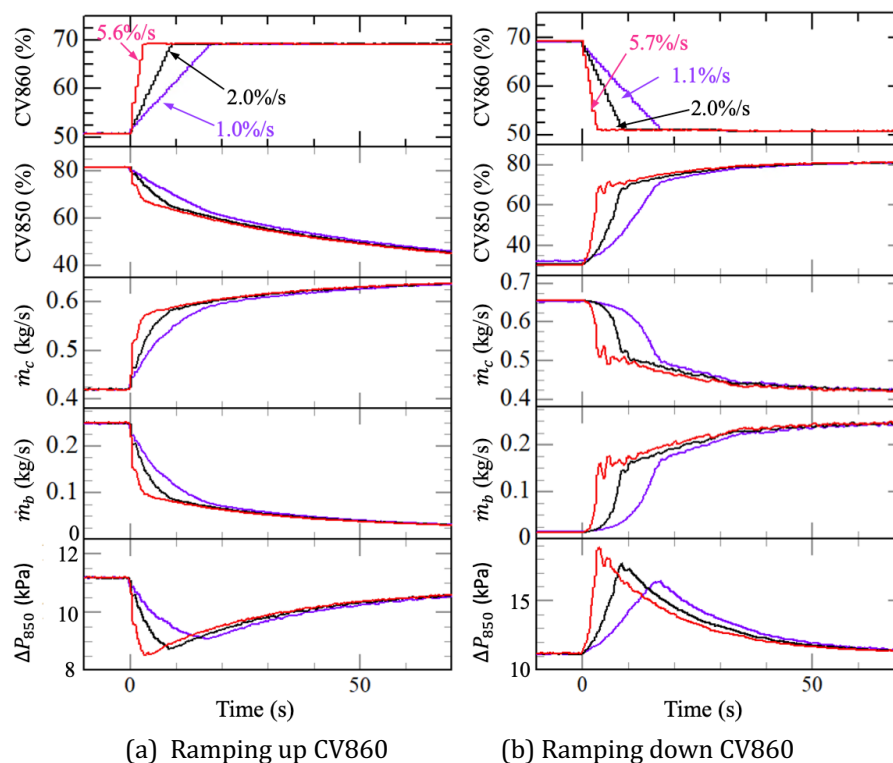


Figure 10. the effect of ramp-up and ramp-down speeds of CV860 on \dot{m}_c and \dot{m}_b .

opened to maintain the PDT850 (ΔP_b) at its PID control setpoint although a temporary increase in ΔP_b was observed due to a delay in its PID control response. However, when the bypass flow rate (\dot{m}_b) exceeded the flow rate delivered to the CMS (\dot{m}_c), oscillation in CV850 were observed. The test results revealed that the upper limit of \dot{m}_b , corresponding to a CV860 position of approximately 87.7%, was equivalent to half of the flow rates through the S-CTL (\dot{m}_s) to prevent such oscillations, consistent with relationship $\dot{m}_s = \dot{m}_c + \dot{m}_b$. Helium discharge pressures (HP) of 0.77 and 1.1 MPa, respectively, were required to achieve the required flow rate (\dot{m}_c) of 0.356 kg/s and 0.452 kg/s under 2 MW and 5 MW proton beam conditions. These pressures also satisfied the required flow rate changes of 0.156 kg/s and 0.252 kg/s, which were necessary to compensate for the dynamic heat load variations. Furthermore, although the maximum ramp speed of CV860 was limited to 5.6%/s due to the actuator's movement capability, it was sufficient for CV860 to operate within the required flow rate ramping ranges of 0.03 to 0.08 (kg/s)/s for 2 MW proton beam operation and 0.06 to 0.09 (kg/s)/s for 5 MW operation.

References

- [1] Garoby R and Danared H et al 2018 *Phys. Scr.* **93** 014001
- [2] Bessler Y, Henkes C, Hanusch F, Schumacher P, Natour G, Butzek M, Klaus M, Lyngh D and Kickulies M 2017 *IOP Conf. Ser: Mater. Sci. Eng.* **171** 012131
- [3] Tatsumoto H, Lyngh D, Bessler Y, M Klaus, Hanusch F, P Arnold and H Quack 2019 *IOP Conf. Ser: Mater. Sci. Eng.* **755** 012101
- [4] Arnold P, Hess W, Jurns J, Su X T, Wang X L and Weisend II J G 2015 *IOP Conf. Ser: Mater. Sci. Eng.* **101** 012011
- [5] Ganni V and Knudsen P 2010 *Adv. Cry. Eng.* **55** pp 1057-71
- [6] Tatsumoto H, Arnold P, Boros M and Horvath A 2024 *IOP Conf. Ser.: Mater. Sci. Eng.* **1301** 13011131.
- [7] Tatsumoto H, P Arnold, M Boros and A. Horvath 2024 *IOP Conf. Ser.: Mater. Sci. Eng.* **1301** 13011126.
- [8] Tatsumoto H, Horvath A, Arnold P, 2025 *IOP Conf. Ser.: Mater. Sci. Eng.* **1327** 012009.